

Despeckling of SAR Images Based on Bayes Shrinkage Thresholding in Shearlet Domain

J.Sivasankari^{#1}, M.Maritta Ashlin^{#2}, T.Janani^{#3}, D.Farehin Shahin^{#4}

^{#1} Faculty, ECE, Ultra College of Engineering and Technology for Women, Tamilnadu, India

^{#2} Students, ECE, Ultra College of Engineering and Technology for Women, Tamilnadu, India

^{#3} Students, ECE, Ultra College of Engineering and Technology for Women, Tamilnadu, India

^{#4} Students, ECE, Ultra College of Engineering and Technology for Women, Tamilnadu, India

ABSTRACT—Synthetic Aperture Radar (SAR) is widely used for obtaining high-resolution images of the earth. SAR Image processing is greatly affected by speckle noise. The despeckling process of SAR image where speckle may interfere with automatic interpretation, which can further affect the processing of SAR image. Synthetic Aperture Radar (SAR) image is easily polluted by speckle noise. The speckle reduction of SAR images is based on spatial filter, Wavelet transform, Curvelet Transform, where the smoothening of image is difficult to achieve. In order to achieve an improvised quality in image the despeckling is done by using shearlet Domain. This project introduces the effective speckle reduction of SAR images based on a new approach of Discrete Shearlet Transform with Bayes Shrinkage Thresholding. The shearlet domain turns out to be a powerful tool for image enhancement in fine-structured areas. This model allows us to classify the shearlet coefficients into classes having different degrees of heterogeneity, which can reduce the shrinkage ratio for heterogeneity regions while suppresses speckle effectively to realize both despeckling and detail preservation. The combined effect of soft thresholding in Shearlet Transform works better when compared to the other spatial domain filter and transforms. It also performs better in the curvilinear features of SAR images.

INDEX TERMS—SAR, Despeckling, Curvelet transform, Shearlet domain, Wavelet transform.

I. INTRODUCTION

SYNTHETIC APERTURE RADAR (SAR) plays an important role in military ground surveillance and earth observation. The SAR-systems have been developed for both space and airborne operations. The imaging system of SAR is based on coherence radiation, so SAR images are inherently degraded by multiplicative speckle, which makes them more difficult to analyze and interpret [1][2]. For these reasons, a preliminary processing of real-valued detected SAR images aimed at speckle reduction, or despeckling, is of crucial importance for a number of applications. Such a preprocessing, however, should be carefully designed to avoid spoiling useful information, such as local mean of backscatter, point targets, linear features and textures [3]. Thus, certain methods have been developed to remove speckle from SAR images. They can be generalized into two categories, namely methods applied before and after image formation. The first category consists of the multilook processing performed in the frequency domain. It is applied to reduce speckle by averaging several statistically dependent looks of the same scene during image focusing in the frequency domain. This method enhances the radiometric resolution at the expense of spatial resolution, resulting in blurring [4]. Spatial filtering, such as Lee filter [5], enhanced Lee filter [6], Gamma MAP filter [7], Frost filter [8] and so on, has low computational complexity so the details of SAR images are not preserved effectively. The wavelet transform is able to represent 1-D signals with a high sparsity. However, this is not the case in 2-D signals. Usually 2-D wavelets are produced by the tensor product of 1-D wavelets. In this case, the wavelet

transform can only identify pointwise discontinuities. In other words, the wavelet transform is not capable of diagnosing the direction of any line-shaped discontinuity in the image. In this case, the sparsity reduces when the wavelet transforms are used for image representation but the Gibbs like ringing phenomenon called artifacts occurs. There are various multiscale analysis tools such as curvelet [9], contourlet [10], [11] and Shearlet [12]-[14] which is used to process the image in multidirection. Curvelets take the form of basic elements, which exhibit high directional sensitivity and are highly anisotropic. The curvelet transform therefore represents edges better than wavelets [15] but the smoothing of the image is not achieved, so we go for Shearlet domain which is an affine system with a single generating mother shearlet function parameterized by a scaling, shear, and translation parameter. The shear parameter is capable of capturing the direction of singularities, where the shearlets are highly dimensional and highly directional.

In our method the shearlet domain is considered where the experimental results are used to obtain a higher value of peak signal-to-noise ratio (PSNR) than the existing geometric representations.

II. SYNTHETIC APERTURE RADAR IMAGING

Synthetic aperture radar (SAR) is an active microwave sensor that transmits microwave and detects the wave that is reflected back by the objects. In SAR imaging, the presence of moving targets in the scene causes phase errors in the SAR data and subsequently defocusing in the formed image. The defocusing caused by the moving targets exhibits space variant characteristics, i.e., the defocusing arises only in the parts of the image containing the moving targets, whereas the stationary background is not defocused. The synthetic aperture radar (SAR) is completely different from passive optical sensor which retains both phase and magnitude of the backscattered radar signal. It enables high-resolution, high-contrast observation and accurate determination of topographical features when captured from an airplane or satellite as shown in figure.1, as it makes use of radar waves to gather data about the earth below.

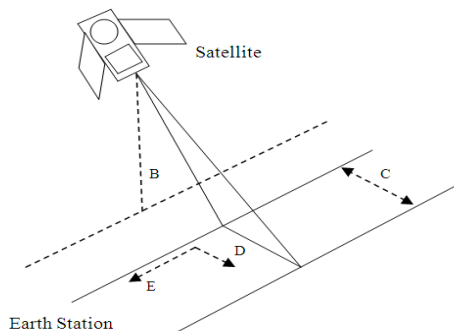


Fig.1 Radar Imaging From Space Borne System

III. IMAGE FORMATION

Image formation modeling, which describes the sequential representation and appearance of objects on an image is represented in figure.2, has been studied for decades, and the basic models can be found in computer vision and image processing books [16], [17]. There are two parts to the image formation process:

1. geometry of image formation
2. physics of light

The geometry of image formation, which determines where in the image plane the projection of a point in the scene will be located and its Geometric parameters are, 1) Type of projections. 2) Position and orientation of camera in space. 3) Perspective distortions introduced by the imaging process. The physics of light, which determines the brightness of a point in the image plane as a function of illumination and surface properties where the photometric parameters are, 1) Type, intensity, and direction of illumination. 2) Reflectance properties of the viewed surfaces.

Traditional image formation modeling describes each specific imaging phenomenon by an individual model such as perspective projection part of an image formation process. Since the image formation process usually involves various geometric and photometric effects, such as defocus blur and vignette, it is often difficult to describe the combined effect by concatenating the individual models. An ordinary image is a projected signal of the light field. With this framework, the transportation of the radiance from the object surface to the image plane can be simply formulated as linear transformations or modulations of the light field which is pictorially represented in figure.3. Furthermore, these various light field manipulations can be combined into a single operation to account for the aggregation of photographic effects [18]. Image Formation occurs when a sensor registers radiation. There are various mathematical models of image formation they are

1. Image function model
2. Geometrical model
3. Radio metrical model
4. Color model
5. Spatial Frequency model
6. Digitizing model

The images which are formed by various mathematical models consist of noise which degrades the quality of the image.

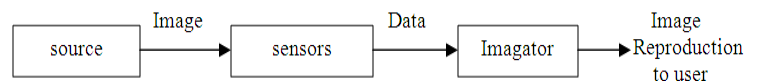


Fig.2 Sequential representation of image formation

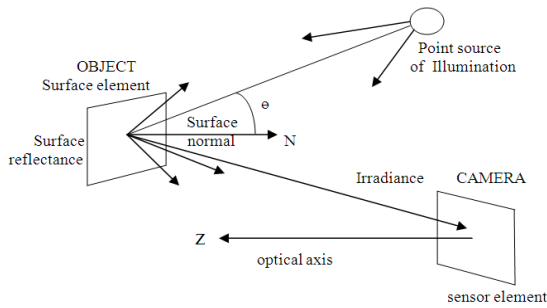


Fig.3 .Model of image formation

IV. IMAGE NOISE

The sources of noise in digital images arise during image acquisition and/or transmission with unavoidable shot noise of an ideal photon detector [19]. The performances of imaging sensors are affected by a variety of factors during acquisition, such as Environmental conditions during the acquisition, Light levels, and Sensor temperature. Depending on the specific noise source, there are different types of noises

- Gaussian noise
- Salt-and-pepper noise
- Shot noise
- Speckle noise

A. Gaussian Noise

Gaussian noise is a noise that has its PDF equal to that of the normal distribution, which is also known as the Gaussian distribution. Gaussian noise is most commonly known as additive white Gaussian noise. Gaussian noise is properly defined as the noise with a Gaussian amplitude distribution. Labeling Gaussian noise as 'white' describes the correlation of the noise. It is necessary to use the term "white Gaussian noise" to be precise [20][21].

B. Salt-and-Pepper Noise

Salt and pepper noise is a noise seen on images. It represents itself as randomly occurring white and black dots. An effective filter for this type of noise involves the usage of a median filter. Salt and pepper noise creeps into images in situations where quick transients, such as faulty switching, take place [22].

C. Shot noise

Shot noise or Poisson is a type of electronic noise that occurs when the finite number of particles that carry energy, such as electrons in an electronic circuit or photons in an optical device, is small enough to give rise to detectable statistical fluctuations in a measurement [23].

D. Speckle Noise

An image with speckle noise is considered as a poor quality image. This type of image can lead to inefficient interpretation of data during processing. Speckle noise is caused by signals from elementary scatterers, the gravity-capillary ripples, and manifests as a pedestal image. Several different methods are used to eliminate speckle noise, based

upon different mathematical models of the phenomenon. One method, for example, employs multiple-look processing [24][25]. A second method involves using adaptive and non-adaptive filters on the signal processing. Such filtering also eliminates actual image information as well, in particular high-frequency information, whereas the applicability of filtering and the choice of filter type involves tradeoffs. Adaptive speckle filtering is better at preserving edges and detail in high-texture areas (such as forests or urban areas)[26][27]. Non-adaptive filtering is simpler to implement, and requires less computational power. There are two forms of non-adaptive speckle filtering: one based on the mean and other based upon the median (within a given rectangular area of pixels in the image). The latter is better at preserving edges whilst eliminating noise spikes, than the former is [28] methods.

V. NEED FOR FILTERING

The presence of noise in the SAR images reduces the PSNR value to a greater extent and in order to obtain a higher peak-to-signal noise ratio (PSNR) the filtering process is employed which is done using spatial domain filtering process. The presence of Speckle [29] noise degrades the quality of US and SAR images and thereby reducing the ability of a human observer to discriminate the fine details of diagnostic examination. Images with speckle noise will result in reducing the contrast of image and difficult to perform where the spatial domain filters like Lee filter [5], enhanced Lee filter [6], Gamma MAP filter [7], Frost filter [8] are employed.

VI. SPECKLE NOISE REDUCTION METHOD

The speckle noise model may be approximated as multiplicative and is given by

$$n_{i,j} = n f_{i,j} m_{i,j} + a_{i,j} \tag{1}$$

Where $n_{i,j}$ represent the noisy pixel and $n f_{i,j}$ represent the noisy free pixel, $m_{i,j}$ signify the multiplicative noise and $a_{i,j}$ indicate the additive noise respectively i, j are indices of the spatial locations. Because the effect of additive noise is considerably smaller compared with that of multiplicative noise (1) may be written as

$$n_{i,j} = n f_{i,j} m_{i,j} \tag{2}$$

Logarithmic compression is applied to the envelope detected echo signal in order to fit within the display range [6]. Logarithmic compression affects the speckle noise statistics and it becomes very close to white Gaussian noise. The logarithmic compression transforms multiplicative form in (2) to additive noise form as

$$\log(n_{i,j}) = \log(n f_{i,j}) + \log(m_{i,j}) \tag{3}$$

$$x_{i,j} = y_{i,j} + n_{i,j} \tag{4}$$

The term $(n_{i,j})$ is the noisy image in the medical image after logarithmic compression is denoted as $x_{i,j}$ and the term $\log n_{i,j}, \log m_{i,j}$ these are the noise free pixel and noisy component after logarithmic compression, as $y_{i,j}, n_{i,j}$ respectively. The next step is the computation of wavelet transform of $x_{i,j}$. One of the important issues to be considered in wavelet transform is the choice of the best wavelet function as well as the transformation algorithm. Since we are interested in isolating the speckle noise in the image, the most appropriate wavelet function is one, which its shape looks like the speckle pattern. For this purpose, we computed the average of i and j cross sections of several speckle samples in the logarithmically transformed data. According to this study, the 2D Gaussian function has been found to be the best model fitted to the speckle pattern cross-section.

VII. EXISTING TECHNIQUES

A. Wavelet Transform

Wavelet transform, which is considered as a powerful tool for the despeckling of SAR images, due to its useful properties such as time-frequency localization, multiresolution, sparsity, and decorrelation. Wavelet despeckling filters are exhibiting fairly well performance over the other standard spatial filters.

The multiscale analysis of wavelet based speckle reduction process usually include (1) logarithmic transformation (2) Discrete wavelet transformation (3) Thresholding the wavelet coefficients (4) inverse discrete wavelet transform and (5) exponential transformation [30]. The wavelet transformation is a bit better than spatial domain filters but the effects such as artifacts occurs during processing and the method is not very directional.

A. Curvelet Transform

The approach with curvelet transform reduce speckle noise and enhance edge features and contrast of synthetic aperture radar (SAR) images[31]. Initial curvelet transform [32], [33], which is also called as the first-generation curvelet transform, decomposes the image into subbands, and then, each scale is analyzed by means of a local ridgelet transform. However, this transform needs many steps, such as subband filtering, tiling, and ridgelet transform, which are very complicated. Later efforts found that a new version of fast curvelet is simpler and faster but approach is not very directional and wrap around effect occurs while is processed.

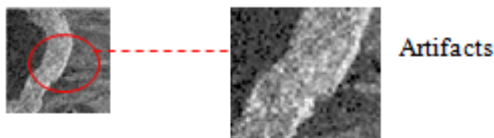


Fig.4 Artifact Effect in Wavelet Transform

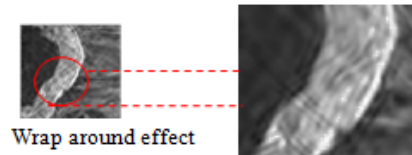


Fig.5 Wrap around Effect in curvelet Transform

VIII. SHEARLET DOMAIN

The shearlet transform is especially designed to address anisotropic and directional information at various scales. Indeed, the traditional wavelet approach, which is based on isotropic dilations, has a very limited capability to account for the geometry of multidimensional functions. In contrast, the analyzing functions associated to the shearlet transform are highly anisotropic, and, unlike traditional wavelets, are defined at various scales, locations and orientations. As a consequence, this transform provides an optimally efficient representation of images with edges[34]. The shearlet transform can be processed in both 2-D and 3-D representations.

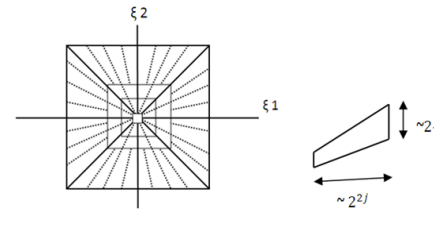


Fig. 5.(a) The tiling of the frequency plane \mathbb{R}^2 induced by the shearlets. The tiling of D_0 is illustrated in solid line; the tiling of D_1 is in dashed line. (b) The frequency support of a shearlet $\psi_{j,l,k}$ satisfies parabolic scaling. The Figure shows only the support for $\xi_1 > 0$; the other half of the support, for $\xi_1 < 0$, is symmetrical.

In this section, we briefly describe a recently developed multiscale and multidirectional representation called the shearlet transform [35]. The collection of discrete shearlets is described by

$$\{\Psi_{j,l,k} = |\det A_0|^{-j/2} (B_0^l A_0^j x - k) : j, l \in \mathbb{Z}, k \in \mathbb{Z}^2\}$$

(5)

Where

$$B_0 = \begin{pmatrix} 1 & 1 \\ 0 & 1 \end{pmatrix}, \quad A_0 = \begin{pmatrix} 4 & 0 \\ 0 & 2 \end{pmatrix}$$

For the appropriate choices of, the discrete shearlets form a Parseval frame (tight frame with bounds equal to $L^2(\mathbb{R}^2)$)[34], i.e., they satisfy the property

$$\sum_{j \in \mathbb{Z}, l \in \mathbb{Z}, k \in \mathbb{Z}^2} \langle x, \Psi_{j,l,k} \rangle^2 = \|x\|^2$$

(6)

The discrete shearlets described above provides a non-uniform angular covering of the frequency plane when restricted to the finite discrete setting for implementation. Thus, it is preferred to reformulate the shearlet transform with restrictions supported in the regions given by

$$D_0 = \{(w_1, w_2) : w_1 \geq 1/8, w_2/w_1 \leq 1\} \text{ And } D_1 = \{(w_1, w_2) : w_2 \geq 1/8, w_1/w_2 \leq 1\}$$

$$\psi^{(0)}(\omega) = \psi_1(\omega) \psi_2\left(\frac{\omega^2}{\omega_1}\right), \psi^{(1)}(\omega) =$$

$$\psi_1(\omega) \psi_2\left(\frac{\omega_1}{\omega^2}\right) \quad (7)$$

where $\psi_1, \psi_2 \in C^\infty(\mathbb{R})$, $\text{supp}\psi_1 \subset [-1/2, -1/16] \cup [1/16, 1/12]$ and $\text{supp}\psi_2 \subset [-1, 1]$

$$\sum_{j \geq 0} |\Psi_1(2^{-2j}\omega)|^2 = 1, \omega \geq \frac{1}{\omega_1} \quad (8)$$

And, for each $j > 0$

$$\sum_{l=-2^j}^{2^j-1} |\Psi_2(2^j\omega - l)|^2 = 1, \omega \leq 1 \quad (9)$$

Let

$$A_1 = \begin{pmatrix} 2 & 0 \\ 0 & 4 \end{pmatrix}, \quad B_1 = \begin{pmatrix} 1 & 0 \\ 1 & 1 \end{pmatrix}$$

Choose to satisfy

$$\phi \in C_0^\infty(\mathbb{R}^2) |\phi(\omega)|^2 + \sum_{d=0}^1 \sum_{j \geq 0} \sum_{l=-2^j}^{2^j-1} |\Psi^{(d)}(\omega A_d^{-j} B_d^{-1})|^2 \chi_{D_d}(\xi) = 1 \quad (10)$$

for $\omega \in \mathbb{R}^2$, where χ_D denotes the indicator function of the set D . with the function ϕ and ψ as above, we deduce the following result.

IX. PROPOSED METHOD

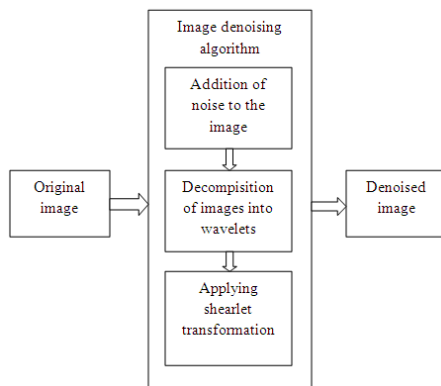


Fig.6 Proposed method adopted for image denoising using Shearlet Transform

a) Peak Signal to Noise Ratio (PSNR)

It is an assessment parameter to measure the performance of the speckle noise removal method [36]. The formula is

$$PSNR = 10 \log_{10} \left(\frac{255 \cdot 255}{MSE} \right) \quad (11)$$

b) Mean Square Error (MSE)

The Mean Square Error is used to find the total amount of difference between two images. It indicates average difference of the pixels throughout the image where DI is the de noised image, and I is the original image with speckle noise. A lower MSE indicates a smaller difference between the original Image with speckle and de noised image [36]. The formula is

$$MSE = \frac{\sum (x, y) - DI \left(\frac{(x,y)^2}{(m \cdot n)} \right)}{x = 1, m, y = 1, n} \quad (12)$$

c) Thresholding Level

We employ Adaptive Bayes Shrinkage threshold On DST Co-efficients,

$$\lambda = \frac{\sigma^2}{\sigma_x} \quad (13)$$

Fig.6 show the proposed method where the DST is applied to get Shearlet co-efficients, then the Bayes shrinkagethresholding was applied using the formula (13), from which hard and soft threshold threshold was calculated to achievebetter result. Moreover performance of the proposed method was analyzed using PSNR and MSE given in formula (11) and (12).

Test Image 1

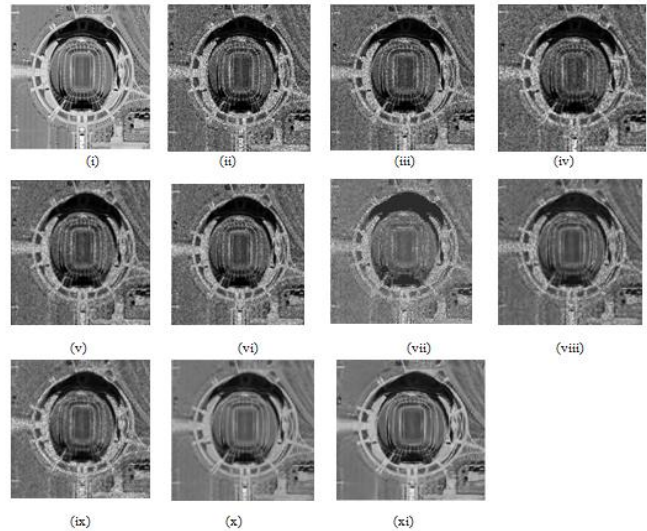


Fig.7 Despeckled Images of Test Image 1by various Methods

Test Image 2

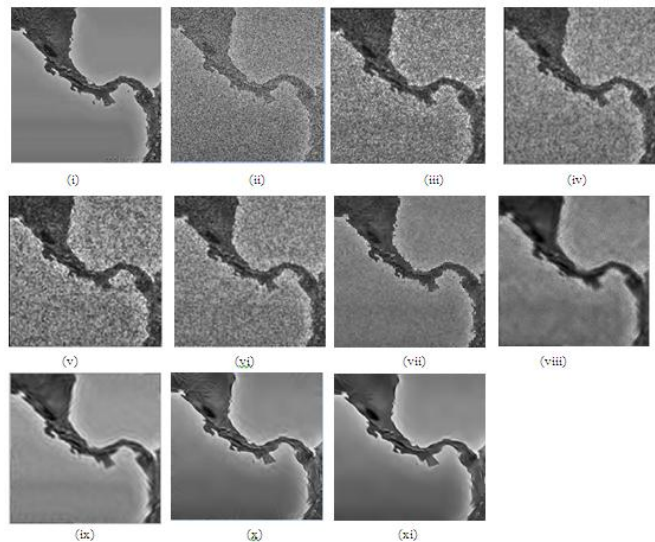


Fig.8 Despeckled Images of Test Image 2 by various Methods

Fig.7&8 (i) Test Image1, Test Image 2(ii) Speckle added image at $\sigma = 20$,

Despeckled image by (iii) Lee filter (iv) Median filter (v) Mean filter (vi) Frost filter (vii) wavelet Transform (viii) Hard threshold in curvelet domain (ix) Soft threshold in curvelet domain (x) Hard threshold in Shearlet Domain (xi) Soft threshold in Shearlet Domain

Table.1 Comparison of MSE & PSNR Values of different despeckling methods for various Test Images

Despeckling Methods	TEST IMAGE 1		TEST IMAGE 2	
	MSE	PSNR	MSE	PSNR
Lee Filter	1180.68	15.71	1830.95	17.53
Median Filter	1059.34	17.30	1403.9	17.51
Mean Filter	847.10	17.64	1172.09	19.65
Frost Filter	773.87	19.25	1188.07	21.16
Wavelet Transform	677.81	25.58	993.19	25.01
Hard Threshold in Curvelet Transform	365.05	28.57	784.46	27.68
Soft Threshold in Curvelet Transform	246.76	30.57	457.34	29.68
Hard Threshold in Shearlet Transform	145.89	35.67	345.78	33.67
Soft Threshold in Shearlet Transform	89.53	39.53	164.74	35.27

Table 1 shows the comparison of PSNR and MSE values of the two test images, from which we can say that the proposed method outperforms all the other method in terms of higher values. Also from the Fig.7 & 8 the visual quality of the despeckled image can be studied that the proposed method overcomes the drawback of the existing techniques and also gives good visual impact in terms of image features when compared to all other techniques.

IX.CONCLUSION AND FUTURE WORK

A sub band dependent threshold is implemented with DST for removing speckle noise. Image denoising algorithm uses both hard and soft thresholding level to improve smoothness and for better edge preservation. The Bayes Shrinkage thresholding based DST outperforms all the other methods and moreover overcomes the drawback of artifacts in wavelet transform and wrap around effect in curvelet transform. The improved performance of Shearlet has been achieved due to its high directionality along more orientations. To improve the performance further the proposed despeckling method can be combined with any spatial filtering technique.

REFERENCES

- [1] Biao Hou, Xiaohua Zhang, Xiaoming Bu, and Hongxiao Feng, "SAR Image Despeckling Based on Nonsubsampled Shearlet Transform" IEEE journal of selected topics in applied earth observations and remote sensing, vol. 5, no. 3, June 2012.
- [2] Oliver and S. Quegan, "Understanding Synthetic Aperture Radar Images". Boston, MA: Artech House, 1998.
- [3] W. Luo, G. L. Heileman, and C. E. Pizano, "JPEG domain watermarking," *Proceedings of SPIE Medical Imaging 2002*, Feb. 2002.
- [4] Hongzhen Chen, Yueting Zhang, Hongqi Wang, and Chibiao Ding, "Stationary-Wavelet-Based Despeckling of SAR Images Using Two-Sided Generalized Gamma Models" *IEEE geoscience and remote sensing letters*, vol. 9, no. 6, November 2012
- [5] J. S. Lee, "Digital image enhancement and noise filtering by use of local statistics," *IEEE Trans. Pattern Anal. Mach. Intell.*, vol. 2, no. 2, pp. 165–168, Mar. 1980.
- [6] Lopès, R. Touzi, and E. Nezry, "Adaptive speckle filters and scene heterogeneity," *IEEE Trans. Geosci. Remote Sens.*, vol. 28, no. 6, pp. 992–1000, Nov. 1990.
- [7] A. Lopès, E. Nezry, R. Touzi, and H. Laur, "Maximum a posteriori speckle filtering and first order texture models in SAR images," in *Proc. IGARSS*, Washington, DC, May 1990, vol. 3, pp. 2409–2412.
- [8] V. S. Frost, J. A. Stiles, K. S. Shanmugan, and J. C. Holtzman, "A model for radar images and its application to adaptive digital filtering of multiplicative noise," *IEEE Trans. Pattern Anal. Mach. Intell.*, vol. 4, no. 2, pp. 157–166, Mar. 1982.
- [9] E. J. Candès and D. L. Donoho, "New tight frames of curvelets and optimal representations of objects with piecewise C2 singularities," *Comm. Pure and Appl. Math.*, vol. 57, no. 2, pp. 219–266, Feb. 2004.
- [10] M. N. Do and M. Vetterli, "The Contourlet transform: An efficient directional multiresolution image representation," *IEEE Trans. Image Process.*, vol. 14, no. 12, pp. 2091–2106, Dec. 2005.
- [11] F. Argenti, T. Bianchi, G. M. di Scarfizzi, and L. Alparone, "LMMSE and MAP estimators for reduction of multiplicative noise in the nonsubsampled contourlet domain," *Signal Process.*, vol. 89, no. 10, pp. 1891–1901, Oct. 2009.
- [12] G. Kutyniok and D. Labate, "Resolution of the wavefront set using continuous shearlets," *Trans. Amer. Math. Soc.*, vol. 361, no. 5, pp. 2719–2754, May 2009.
- [13] G. Easley, D. Labate, and W. Lim, "Sparse directional image representations using the discrete Shearlet transform," *Appl. Comput. Harmon. Anal.*, vol. 25, no. 1, pp. 25–46, Jan. 2008.
- [14] G. Kutyniok and T. Sauer, "From wavelets to Shearlets and back again," in *Approximation Theory XII (San Antonio, TX, 2007)*. Nashville, TN: Nashboro Press, 2008, pp. 201–209.
- [15] Ying Li, Hongli Gong, Dagan Feng, and Yanning Zhang, "An Adaptive Method of Speckle Reduction and Feature Enhancement for SAR Images Based on Curvelet Transform and Particle Swarm Optimization" *IEEE transactions on geoscience and remote sensing*, vol. 49, no. 8, August 2011
- [16] B. K. P. Horn, *Robot Vision*. Cambridge, MA: MIT Press, 1986.
- [17] R. Hartley and A. Zisserman, *Multiple View Geometry in Computer Vision*, 2nd ed. Cambridge, U.K.: Cambridge Univ. Press, 2003.
- [18] Chia-Kai Liang, Yi-Chang Shih, and Homer H. Chen "Light Field Analysis for Modeling Image Formation" *IEEE TRANSACTIONS ON IMAGE PROCESSING*, VOL. 20, NO. 2, FEBRUARY 2011
- [19] Jaideva Goswami Andrew K. Chan, "Fundamentals Of Wavelets Theory, Algorithms, And Applications", John Wiley Sons

- [20] M. Sonka, V. Hlavac, R. Boyle *Image Processing, Analysis, and Machine Vision*. Pp10-210 & 646-670
- [21] S. Poornachandra/ "Wavelet-based denoising using subband dependent threshold for ECG signals" / *Digital Signal Processing* vol. 18, pp. 49–55 / 2008
- [22] Charles Bonchelet (2005). "Image Noise Models". in Alan C. Bovik. *Handbook of Image and Video Processing*.
- [23] Arthur Jr Weeks, *Fundamental of Electronic Image Processing*
- [24] Tinku Acharya, Ajoy K. Ray, "*image processing – principles and applications*", Hoboken, New Jersey, John Wiley & Sons, Inc., publication, 2005
- [25] S. Poornachandra/ "Wavelet-based denoising using subband dependent threshold for ECG signals" / *Digital Signal Processing* vol. 18, pp. 49–55 / 2008
- [26] Raghuveer M. Rao., A.S. Bopardikar *Wavelet Transforms: Introduction To Theory And Application Published By Addison-Wesley* 2001 pp1-126
- [27] M. R. Banham, "*Wavelet-Based Image Restoration Techniques*", Ph.D. Thesis, Northwestern University, 1994.
- [28] J. W. Goodman, "Some fundamental properties of speckle," *J. Opt. Soc. Amer.*, vol. 66, no. 11, pp. 1145–1149, 1976.
- [29] Portilla, J., Strela, V., Wainwright, M., Simoncelli E.P., "*Image Denoising using Gaussian Scale Mixtures in the Wavelet Domain*", TR2002-831, Computer Science Dept, New York University. 2002.
- [30] R. Sivakumar, Member, M. K. Gayathri and D. Nedumaran, "*Speckle Filtering of Ultrasound B-Scan Images- A Comparative Study of Single Scale Spatial Adaptive Filters, Multiscale Filter and Diffusion Filters*"
- [31] Ying Li, Hongli Gong, Dagan Feng and Yanning Zhang "An Adaptive Method of Speckle Reduction and Feature Enhancement for SAR Images Based on Curvelet Transform and Particle Swarm Optimization" *IEEE transactions on geoscience and remote sensing*, vol. 49, no. 8, August 2011
- [32] E.J. Candès and D. L. Donoho, "Curvelets—A surprisingly effective nonadaptive representation for objects with edges," in *Curve and Surface Fitting: Saint-Malo 1999*, A. Cohen, C. Rabut, and L. L. Schumaker, Eds. Nashville, TN: Vanderbilt Univ. Press, 1999.
- [33] E. J. Candès and D. L. Donoho, "Recovering edges in ill-posed inverse problems: Optimality of curvelet frames," *Ann. Statist.*, vol. 30, no. 3, pp. 784–842, Jun. 2002.
- [34] K. Guo and D. Labate, "Optimally sparse multidimensional representation using shearlets", *SIAM J. Math. Anal.*, Vol.9, pp. 298–318, 2007
- [35] G. R. Easley, D. Labate, and W.-Q. Lim, "Sparse directional image representations using the discrete shearlet transform," *Appl. Comput. Harmon. Anal.*, vol. 25, no. 1, pp. 25–46, Jul. 2008.
- [36] T. Ratha, Jeyalakshmi and K. Ramar "Modified Method for Speckle Noise Removal in Ultrasound Medical Image" *International Journal of Computer and Electrical Engineering*, Vol. 2, No. 1, February, 2010
- [37] K. Guo, W. Lim, D. Labate, G. Weiss, and E. Wilson, "Wavelets with composite dilations and their MRA properties," *Appl. Comput. Harmon. Anal.*, vol. 20, pp. 231–249, 2006.